Research Journal of Recent Sciences _____ ISSN 2277-2502
Vol. 4**(ISC-2014),** 131-135 **(2015)** *Res. J. Recent. Sci.*

UV- Visible, Mechanical and Anti-Microbial Studies of Chitosan - Montmorillonite Clay / TiO_2 Nanocomposites

V. Vijayalekshmi*
Dept of Chemistry, S.N College for Women, Kollam, Kerala, 691001, INDIA

Available online at: www.isca.in, www.isca.me
Received 30th November 2014, revised 26th January 2015, accepted 23rd February 2015

Abstract

The development of bio-based nanocomposites are carried out with the intention of providing physical protection for food, improving food integrity, and preventing contamination from microbes and fungi [1,2]. Nanocomposites of chitosan, nanoclay (MMT-Na^+) and Titanium dioxide (TiO_2) were prepared. The UV- Visible analysis of the samples was carried out using UV-Visible Spectrophotometer. Maximum absorbance was observed at 362 nm for 5weight percentage (wt%) MMT and 0.8 TiO_2 loading. From the Tauc,s plot, it was observed that the optical band gap was found to be in the range of 2.9 to 2.2 eV. The refractive index of the material was also calculated. The structural properties were studied using X-ray diffraction (XRD) Transmission electron microscopy (TEM) and Scanning electron microscopy (SEM). XRD and TEM results indicated that an exfoliated structure was formed by the addition of small amount of filler. Antibacterial activity was investigated using gram-negative bacteria and gram- positive bacteria. All have high antibacterial activity. The 30% increase in tensile strength was observed in the case of 5wt% nanofiller loading.

Keywords: Chitosan, TiO_2, montmorillonite, nanocomposites.

Introduction

Polymeric materials have been used for a wide range of industrial applications in packaging and protective coatings[1]. The use of biopolymers as components of composites for packaging materials is very popular due to the remarkable improvement in properties such as biodegradable, antimicrobial, mechanical, thermal and low swelling properties when compared to pure organic polymers[2]. Reinforcing polymer with nanosized fillers yield materials with enhanced performance[3-5]. In the past two decades, titanium dioxide (TiO_2) has wide applications on multidisciplinary areas due to its excellent properties such as nontoxic[6], ultraviolet (UV) blocking and protection[7-10]. In this paper, the effect of nanoclay and TiO_2 content on the structural, morphological, mechanical, UV-Vis and antimicrobial properties of Ch-MMT/TiO_2 composite films was investigated.

Material and Methods

Materials: Chitosan (Ch) of medium molecular weight (average molecular weight M=92,700 g/mol^{-1}), used in this work was brought from Aldrich Chemicals. This chitosan was obtained by deacetylation of chitin from crab shells and it had a degree of deacetylation of 82.5%. Glacial acetic acid (HAc) obtained from Aldrich Chemicals was used as solvent for chitosan. The unmodified pristine montmorillonite (MMT), with a cationic exchange capacity (CEC) of 92.6meq/100g, was supplied by Southern clay products Inc., USA. Glycerol and titanium dioxide (TiO_2) were obtained from Sigma Aldrich.

Preparation of nanocomposites: Ch/MMT-Na^+/TiO_2 nanocomposites: A solution of chitosan (Ch) were made by dissolving 4g chitosan in 1% (v/v) aqueous acetic acid solution and thereafter centrifuged to discard the unsolvable substance[2]. The dispersed MMT-Na^+ in 50ml distilled water was then poured in to 50ml chitosan solution with MMT-Na^+ composition of 1wt%, 3wt%, 5wt% and 7wt% and TiO_2 in the order of 0.7, 0.8, 1 and 1.5wt% and followed by stirring at 40^0C for 48hrs. The particle size of TiO_2 is found to be 15 nm. The glycerol contents were optimized at a level of 0.7wt%. Pure Ch films and its nanocomposites were dried at room temperature. Clay composition and TiO_2 composition were optimized. Studies were done using 5wt% clay and 0.8wt% TiO_2 loading.

XRD, SEM and TEM: X-ray diffraction (XRD) was used to study the nature and extend of dispersion of clay filled sample. XRD were collected by using Rigaku D-Max using Cu Kα (λ =1.5418 A^0) diffractometer. The polymer nanocomposite samples were scanned in step mode by 1.0 ^{0}/min scan rate in the range of 2θ<12 ^{0}. The samples of 1x1 cm sheets were used for the characterization. Scanning electron microscopic studies of samples were carried out on a freshly cut surface in a JSM-6400 scanning microscope, JEOL. The sample surface were gold plated before examination. The microscopy was performed using a JEOL, JEM -2010 (Japan), TEM operating at an accelerating voltage of 200 kV. The composite samples were cut by ultra-cyromicrotomy using a Leica Ultracut UCT. Freshly sharpened glass knives with cutting edge of 45^0 were used to get the cryosections of 50-70 nm thickness. Since these samples were elastomeric in nature, the temperature during ultra cryomicrotomy was kept at -70^0C (which was below the glass

transition temperature of EVA). The cryosections were collected individually on sucrose solution and directly supported on copper grid of 300-mesh size.

UV- Visible spectroscopy: The UV- Visible analysis of the samples was carried out using UV- Visible Spectrophotometer. UV- Visible Perkin Elmer Spectrophotometer (Lamda-850) was used to obtain the spectra of the samples. Information were recorded in the absorbance mode in the wavelength choice of 200-800nm.

Antibacterial properties: Antibacterial activity of the material was determined against Gram positive bacteria Bacillus cereus and Gram negative bacteria E.Coli. It was assayed by so called halo method. A melted beef agar medium was poured into a Petri dish and solidified. Then, the medium containing bacteria ($1x10^6$ cells of E.coli, Bacillus cereus per ml) was layered over it. The samples were poured into a well cut on the surface then incubated for one day at 37^0C. Samples having antibacterial activity show a halo circle along the outside edge of the sample. The halo ring formed will be very broad in the case of samples having high antibacterial activity.

Tensile Properties: Tensile properties of the samples were determined with an Instron Universal Testing Machine (model 5565, Instron Engineering Corp grip. The separation of the grip was set at 50 mm, and also a cross-head speed of 50 mm/min. The tensile strength and elongation measurements were done with seven specimens cut from each sheet of film; thus, the measurements were done on a total of 7 specimens per each film type, with the mean values for TS and E for a single sample.

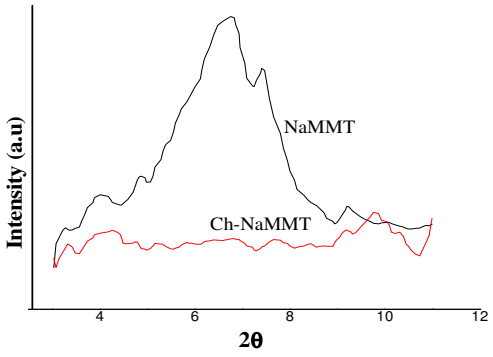

Figure-1
XRD pattern of the nanocomposites

Results and Discussion

XRD: Figure - 1 shows the XRD pattern of MMT-Na^+ and nanocomposite with 5wt% clay loading. The MMT-Na^+ filler exhibits a peak at an angle of 2θ of 7.2^o corresponding to a basal spacing $12.26A^0$. For chitosan based nanocomposites with 5 wt% NaMMT clay and 0. 8 TiO_2 content, the 2 theta shifts to a lower value 4.3^0 that is assigned to an interlayer spacing of 20.5 A^0. This may be due to the better interaction between Na^+ ions of the Na-MMT and the free hydroxyl groups of chitosan. This biopolymer has good miscibility with MMT and can easily intercalate into the interlayer by means of cationic exchange due to the hydrophilic and polycationic nature of chitosan in acidic media.

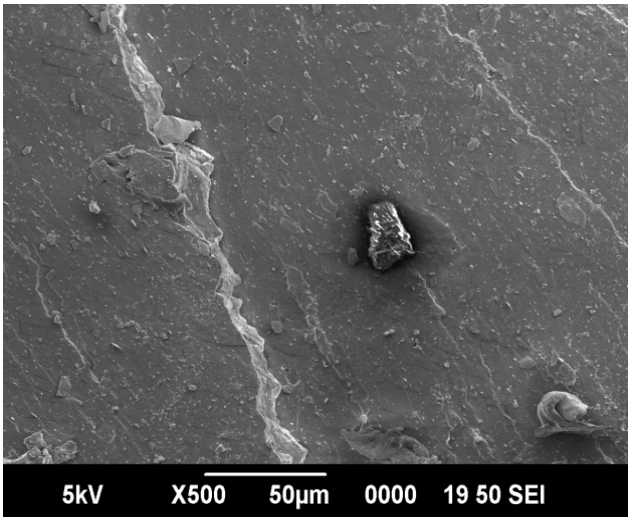

Figure-2(a)
Pure Chitosan

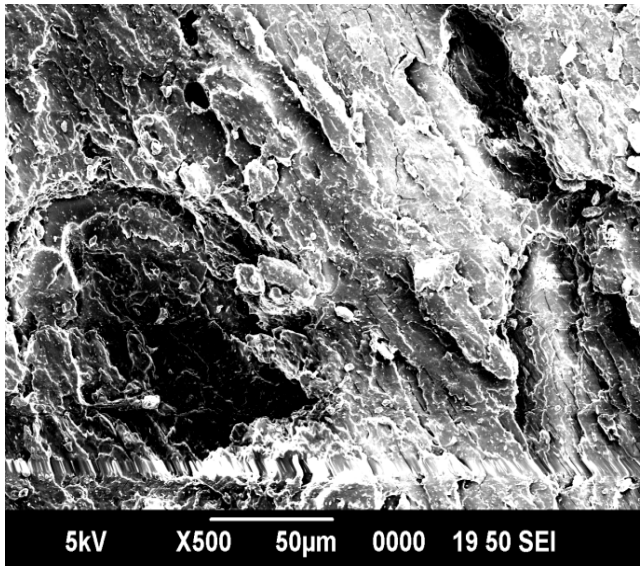

Figure-2(b)
Ch with 5wt% NaMMT and 0.8 TiO_2 loading

SEM Images: Figure 2 (a) and (b) shows the SEM images of pure Ch and 5wt% clay loaded nanocomposites. From the images (a) and (b) it is clear that the particles are well dispersed into the chitosan matrix.

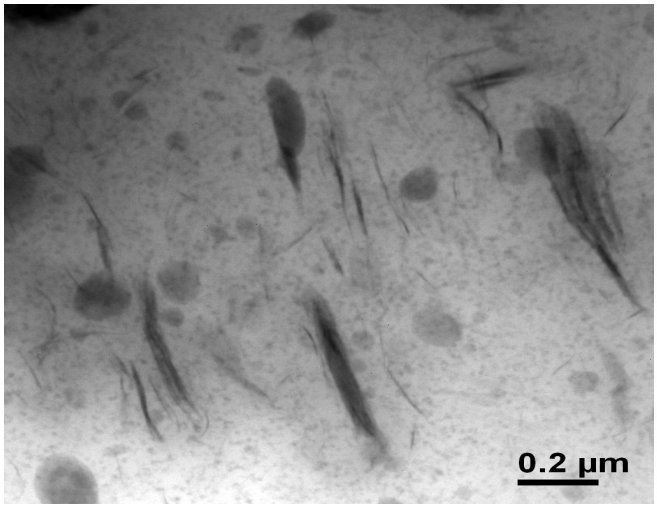

Figure-3
Ch- Na MMT/TiO_2 nanocomposite with 5 and 0.8wt% filler loading

TEM images: Figure- 3 shows the TEM images of nanocomposites with 5wt% clay + 0.8 TiO_2 loading. Partially intercalated and exfoliated structure is observed for the nanocomposites, which clearly reveals better dispersion of filler within the chitosan matrix.

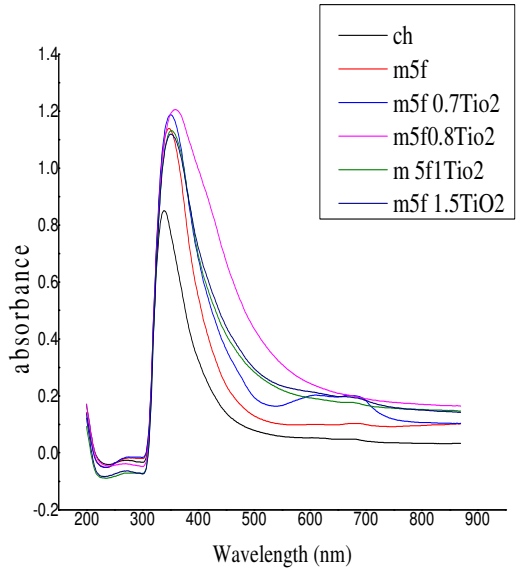

Figure-4
Shows the UV absorption spectrum of Chitosan and 5wt% clay loaded nanocomposites

UV-Visible spectra: The UV spectrum of the sample at room temperature with 1 nm resolution is shown in figure- 4. An absorption band were observed in the 300-400nm. The wavelength of chitosan and its nanocomposites were found to be 339 nm and 361nm respectively.The band at 300-400nm gives the absorption which is related to the direct electronic d-π^* orbitals and is called the Soret band. The UV absorption spectrum of Chitosan and its nanocomposites are shown in figure- 4. From this it is clear that the absorption is maximum for the 5wt% clay and 0.8wt% TiO_2 filled sample.

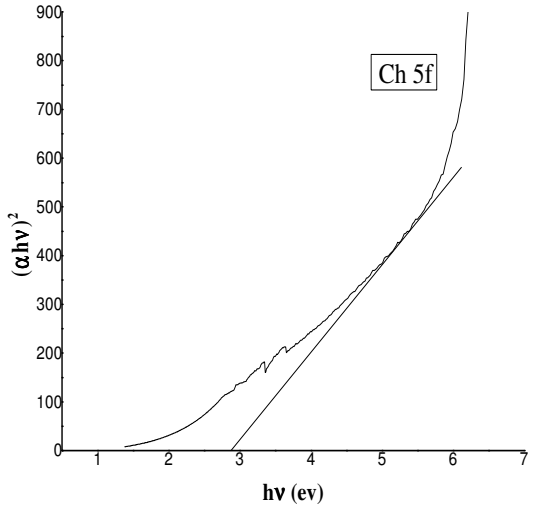

Figure-5(a)
Tauc's plot of pure Ch

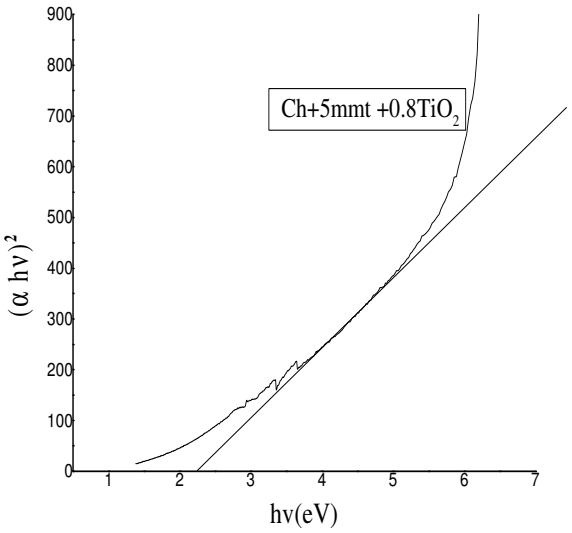

Figure-5(b)
Tauc's plot of Ch nanocomposites

Tauc's plot: In the figure 5 (a), Ch shows a band gap of 2.9 eV and in figure 5(b) Ch nanocomposites shows a band gap of 2.2 eV which indicates that nanocomposites shows an improved conducting property when compared to pure matrix. The refractive index of the material was found to be in between 1.12 and 2.26.

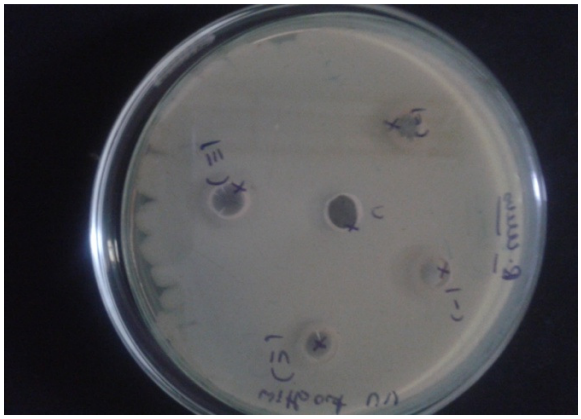
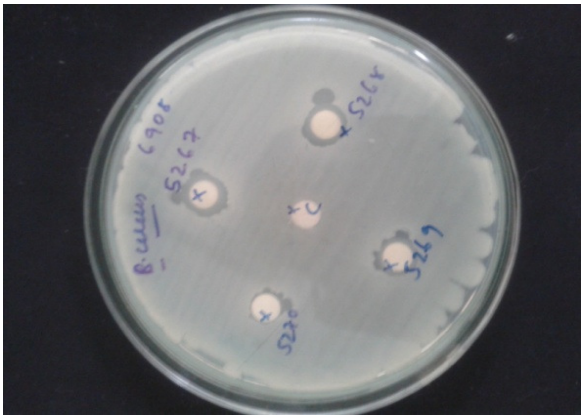

Figure-6 (a) and 6 (b)
Shows the antibacterial assessment of chitosan and its nanocomposites with different clay loading against Bacillus cereus without and with UV irradiation

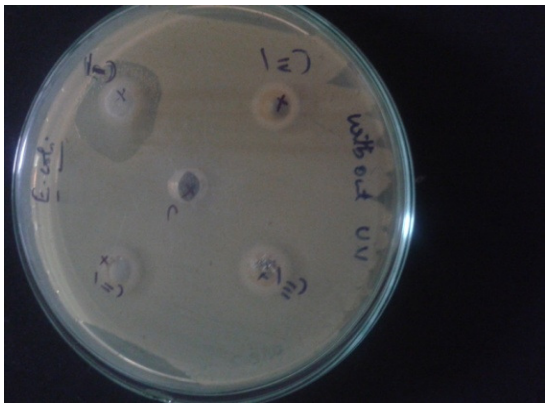
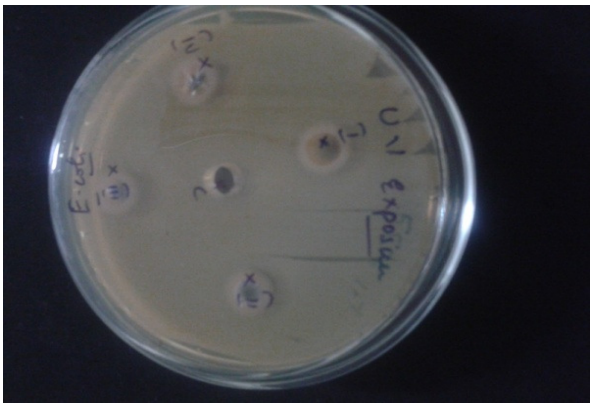

Figure-6(c) and 6(d)
shows the antibacterial assessment of chitosan and its nanocomposites with different clay loading against Escherichia coli without and with UV irradiation

Antibacterial properties: The organoclay nanocomposites posses antibacterial property against both Gram negative bacteria and Gram positive bacteria. More antibacterial property is exhibited by gram negative bacteria. Although the mode of action of cations against bacteria is not known, it was suggested that an adsorption of cations onto the negatively charged cell surface by electrostatic interaction. In Bacillus cereus, the UV irradiated sample is more resistant to bacterial attack when compared to unirradiated sample. In the case of E-coli, the unirradiated sample shows a better antibacterial property when compared to UV irradiated sample.

Table-1
Halo ring diameter obtained from antibacterial assessment

Samples	E.coli (mm)	Bacillus cereus (mm)
Chitosan (Ch)	4	6
Ch + 1%Na^+ +0.8TiO_2	7	9
Ch + 3%Na^+ +0.8 TiO_2	17	10
Ch + 5%Na^+ +0.8 TiO_2	20	16

Table-2
Tensile properties of chitosan and its nanocomposite films

Film type	Tensile strength (MPa)	Modulus at 300% elongation (MPa)	Elongation at Break (%)
Chitosan (Ch)	32.4	1.68	59
Ch+Na-MMT 1% + 0.8% TiO_2	35.2	2.23	54
Ch+Na-MMT 3% + 0.8% TiO_2	36.9	2.56	53
Ch+Na-MMT 5% +0.8% TiO_2	38.2	2.98	51
Ch+Na-MMT 7% + 0.8% TiO_2	36.5	2.71	52

Tensile Properties: The enhanced modulus and tensile strength observed reflect a direct result of the better polymer- filler interaction.

Conclusion

The 2θ value and d-spacing of nanocomposites decreased by 2.9^0 and increased by $7.74A^0$ respectively. From the SEM images it is observed that particles are uniformely dispersed, which means a better interaction between the filler and the matrix. A partially intercalated and exfoliated structure is observed from TEM images. A better UV absorption property is observed for nanocomposites when compared to the pure matrix. The wavelength of Ch and nanocomposites are found to be 339 nm and 361nm respectively. Optical band gap decreases by the addition of nanofiller loading. An enhancement in conducting property is observed for nanocomposites, which is evident from Tauc's plot. Antibacterial activity of Chitosan and its nanocomposites with varying clay and TiO_2 loading was done with and without UV exposure and showed strong antibacterial activity against Gram-positive and Gram-negative bacteria. The mechanical property shows an increasing trend on the addition of filler.

References

1. Casariego A., Souza B.W.S., Cerqueira M.A., Teixeira J.A., Cruz L., Diaz R. and Vicente A.A., Chitosan/ clay films, properties as affected by biopolymer and clay micro/nanoparticles concentrations, *Food hydrocolloids.,* **23**, 1895-1902 **(2009)**

2. Wang S.F., Shen L., Tong Y.J., Chen L., Phang I.Y., Lim P.Q. and Li T.X., Biopolymer chitosan/montmorillonite nanocomosites: Preparation and characterization, *Polymer Degradation and Stability.,* **90**, 123-131 **(2005)**

3. Pavlidou S. and Papaspyrides C.D., A review on polymer-layered silicate nanocomposites, *Prog. Polym. Sci.,* **33**, 1119-1198 **(2008)**

4. Hu H., Onyebueke L. and Abatan A., Charecterizing and Modeling Mechanical Properties of nanocomposites-Review and Evaluation, *J. of Minerals and Materials Characterization and Engg.,* **9**, 275-319 **(2010)**

5. Kango S., Kalia S., Celli A., Njuguna J., Habibi Y. and Kumar R., Surface modification of inorganic nanoparticles for organic in-organic nanocomposites, *Prog. Polym. Sci.,* **38**, 1232-1261 **(2013)**

6. Sun Q., Sun X., Dong H., Zhang Q. and Dong L., Copper quantum dots on TiO_2: A high-performance, low-cost, and nontoxic photovoltaic material, *J Renewable Sustainable Energy.,* 5, 021413 **(2013)**

7. Carneiro J.O., Teixeira V., Nascimento J.H., Neves J. and Tavares P.B., Photocatalytic activity and UV-protection of TiO2 nanocoatings on poly(lactic acid) fibres deposited by pulsed magnetron sputtering., *Journal of Nanoscience and Nanotechnology,* 11, 8979-85 **(2011)**

8. Seentrakoon B., Junhasavasdikul B. and Chavasiri W., Enhanced UV protection and antibacterial Properties of Natural Rubber/ Rutile TiO_2 - nanocomposites, Polymer Degradation and Stability., 98, 566-78 **(2013)**

9. Kim Y.K. and Min D.H., UV protection of reduced graphene oxide films by TiO_2 Nanoarticle Incorporation, *Nanoscale.,* **5**, 3638-42 **(2013)**

10. Yang H., Zhu S. and Pan N., Studying the mechanisms of Titanium dioxide as ultraviolet-blocking additive for films and fabrics by an improved scheme, *Journal of Applied Polymer Science.,* **92**, 3201-10 **(2004)**